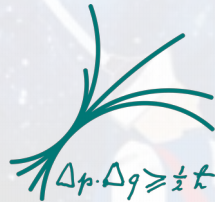


Determination of the strong coupling constant $\alpha_s(m_Z)$ in next-to-next-to-leading order QCD using H1 jet cross section measurements

Daniel Britzger
for the H1 Collaboration and NNLOJET
Eur.Phys.J.C 77 (2017), 791 [arXiv:1709.07251]

ICHEP2018 Seoul
Seoul, Korea
06.07.2018



Max-Planck-Institut für Physik
(Werner-Heisenberg-Institut)



MAX-PLANCK-GESELLSCHAFT



Why α_s ?

Strong coupling α_s enters in the calculation of every process that involves the strong interaction

World average value

$$\alpha_s(m_Z) = 0.1181 \pm 0.0011 \text{ [PDG2016]}$$

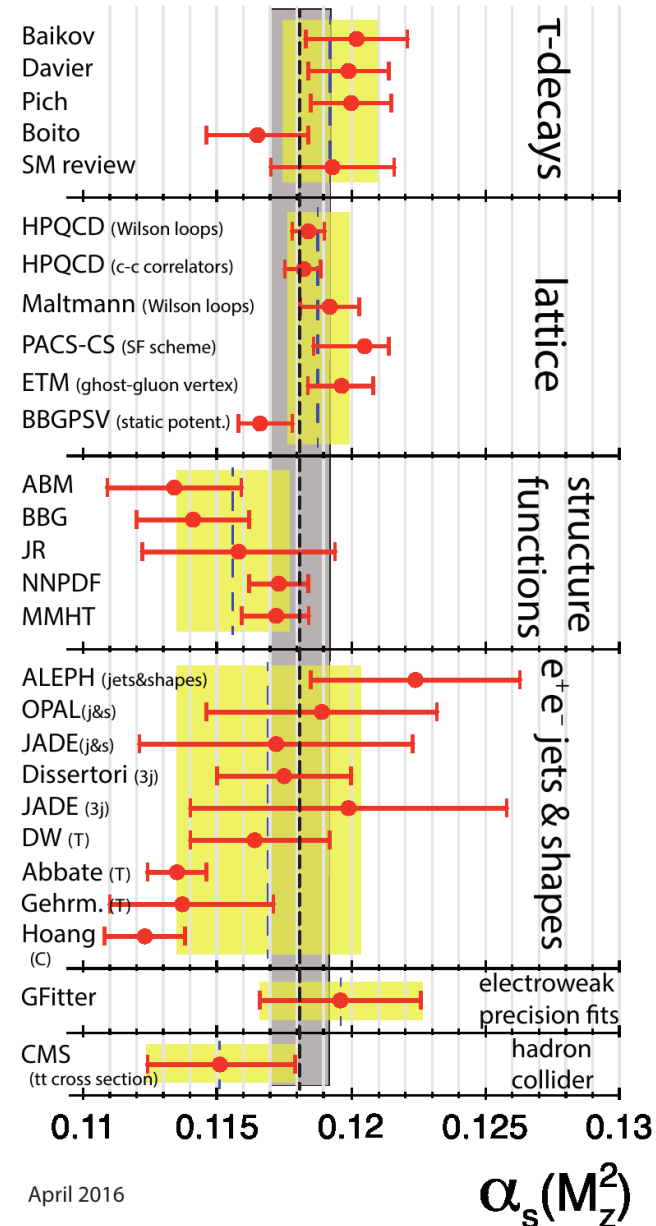
~0.9% relative uncertainty

Uncertainty on α_s

-> non-negligible uncertainties on many observables:
e.g. Higgs production cross sections, branching ratios, ...

Jet measurements

- Direct constraint on α_s
- So far no NNLO results available



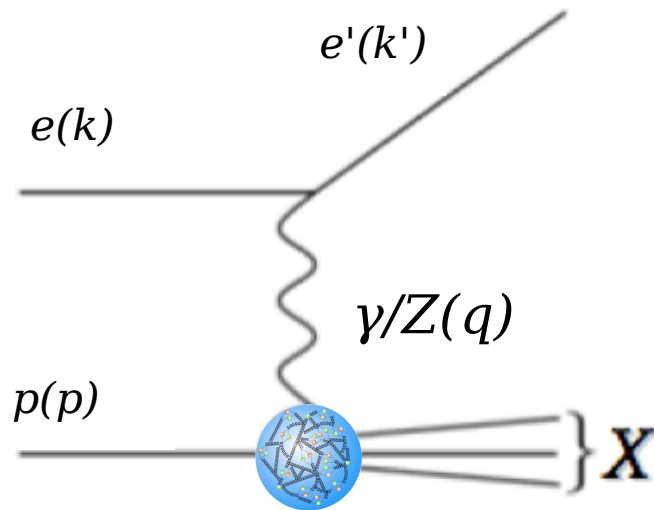
April 2016

$\alpha_s(M_Z^2)$

Deep-inelastic ep scattering

Neutral current scattering (NC)

$$ep \rightarrow e'X$$



Kinematic variables

Photon virtuality

$$Q^2 = -q^2 = -(k - k')^2$$

Inelasticity

$$y = \frac{p \cdot q}{p \cdot k}$$

HERA ep collider in Hamburg



Data taking periods

- HERA I: 1994 – 2000
- HERA II: 2003 – 2007
- $\sqrt{s} = 300$ or 319 GeV

H1 Experiment at HERA

H1 multi-purpose detector

Asymmetric design

Trackers

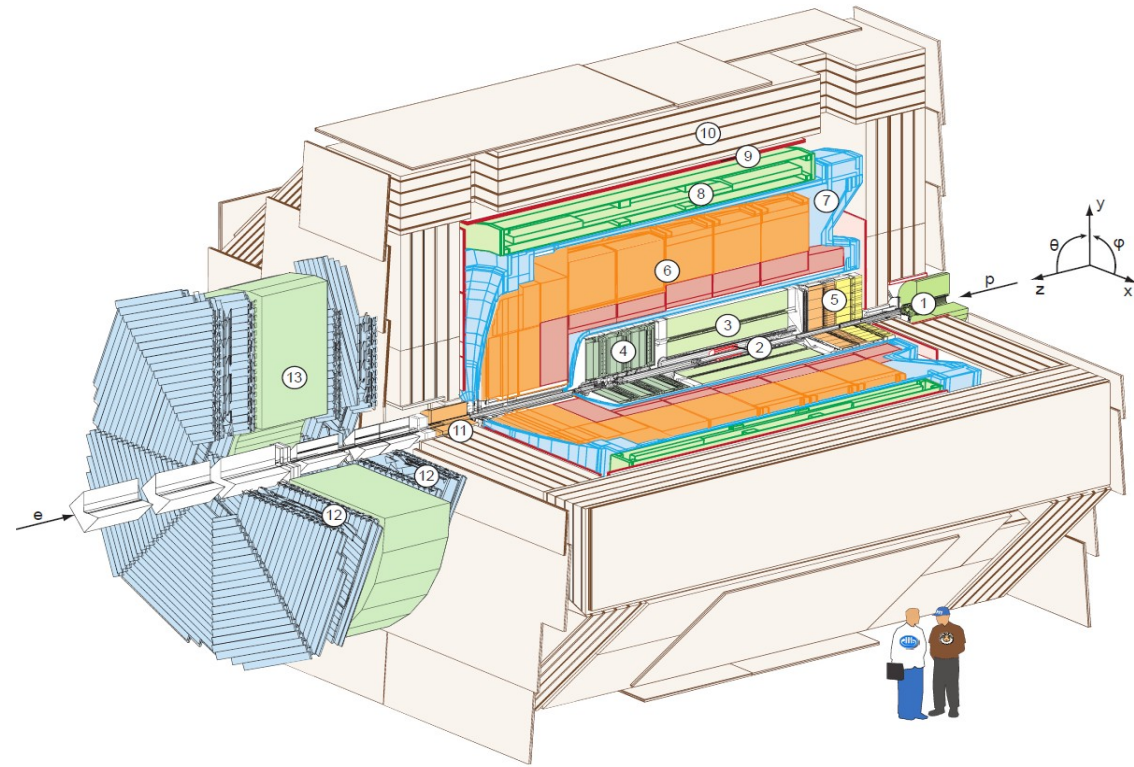
- Silicon tracker,
- Jet chambers
- Proportional chambers

Calorimeters

- Liquid Argon sampling calorimeter
- SpaCal: scintillating fiber calorimeter

Superconducting solenoid, 1.15T

Muon detectors



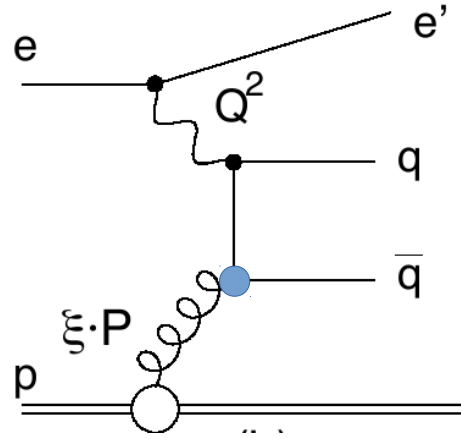
High experimental precision

- Overconstrained system in NC DIS
- Electron measurement: 0.5 – 1% scale uncertainty
- Jet energy scale: 1%

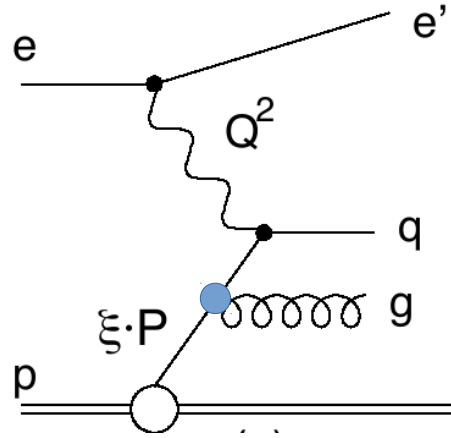


Drawing of the
H1 experiment

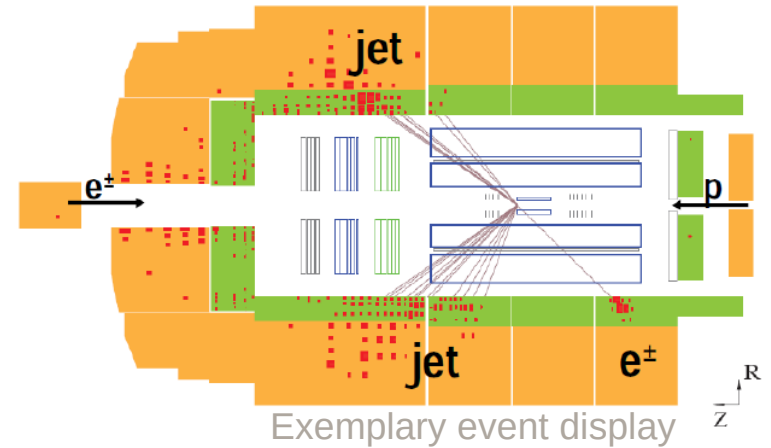
Jet production in DIS



Boson-gluon fusion



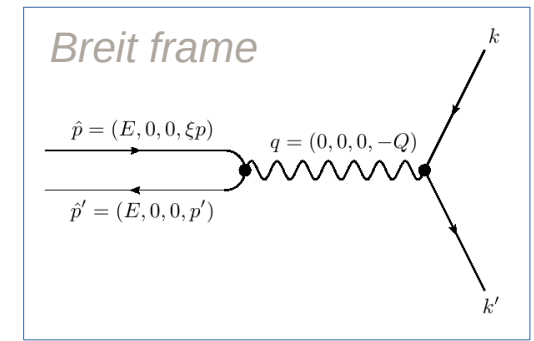
QCD Compton



Jets in DIS measured in Breit frame

- $ep \rightarrow 2\text{jets}$
- Virtual boson collides 'head-on' with parton from proton
- Boson-gluon fusion dominant process
- QCD compton important only for high- p_T jets (high- x)

Jet measurement sensitive to α_s and gluon density



Inclusive jet cross sections by H1

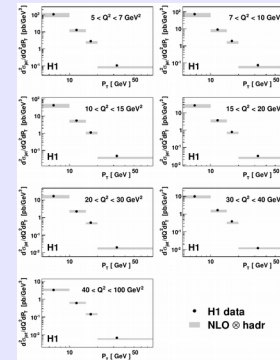
Inclusive jet cross sections

- $d\sigma/dQ^2 dP_{T,jet}$
- 300 GeV, HERA-I & HERA-II
- low- Q^2 ($<100 \text{ GeV}^2$) and high- Q^2 ($>150 \text{ GeV}^2$) regions

Consistency

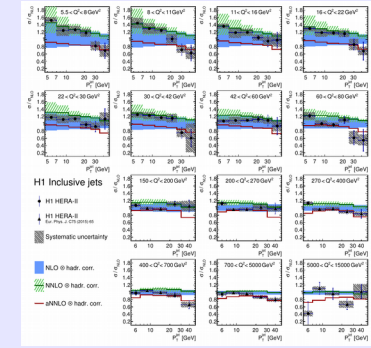
- kt-algorithm, $R=1$
- $-1.0 < \eta < 2.5$
- P_T ranges from 4.5 to 50 GeV

HERA-I low- Q^2



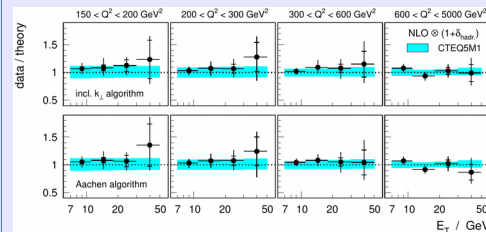
Eur.Phys.J.C67 (2010) 1

HERA-II low- Q^2



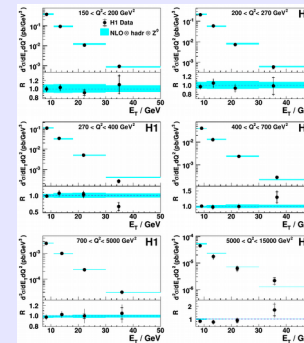
arXiv:1611.03421

300 GeV high- Q^2



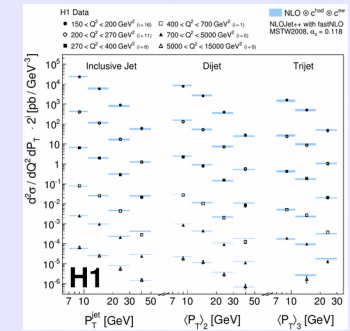
Eur.Phys.J.C19 (2001) 289

HERA-I high- Q^2



Phys.Lett.B653 (2007) 134

HERA-II high- Q^2



Eur.Phys.J.C75 (2015) 2
arXiv:1611.03421

Dijet cross section by H1

Dijet definitions

- $\langle p_T \rangle$ greater than 5, 7 or 8.5 GeV
- P_T jet greater 4, 5 or 7 GeV
- Asymmetric cuts on $p_{T, \text{jet}1}$ and $p_{T, \text{jet}2}$
- M_{12} cut for two data sets

Dijet cross sections

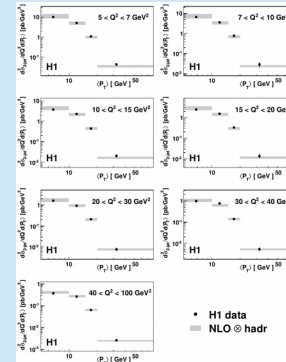
- $d\sigma/dQ^2 d\langle p_T \rangle$
- 300 GeV, HERA-I & HERA-II
- low- Q^2 and high- Q^2

Earlier studies

All inclusive jet and dijet data have been employed for α_s extractions previously

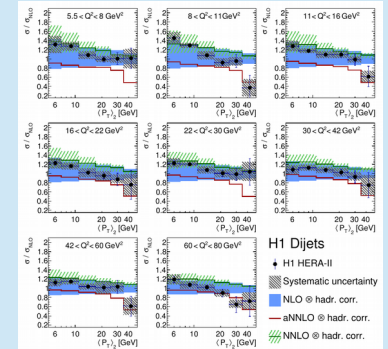
-> Data and uncertainties well-understood
-> NNLO theory is new

HERA-I low- Q^2



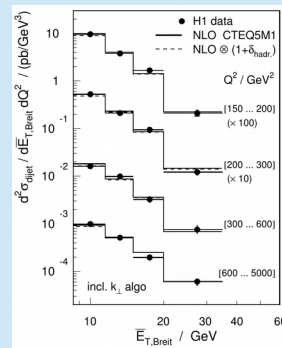
Eur.Phys.J.C67 (2010) 1

HERA-II low- Q^2



Eur.Phys.J. C77 (2017) 215

300 GeV high- Q^2



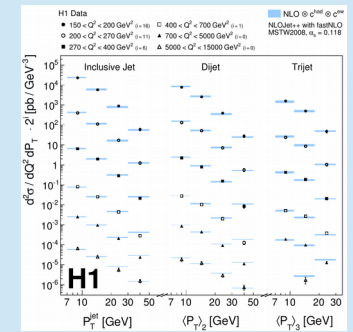
Eur.Phys.J.C19 (2001) 289

HERA-I high- Q^2

Dijet cross sections not statistically independent from HERA-II analysis

Eur.Phys.J.C65 (2010) 363

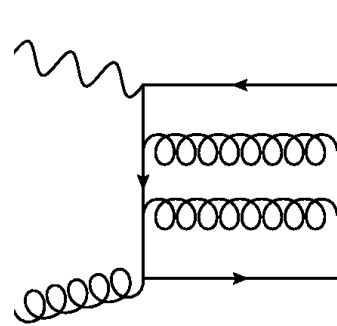
HERA-II high- Q^2



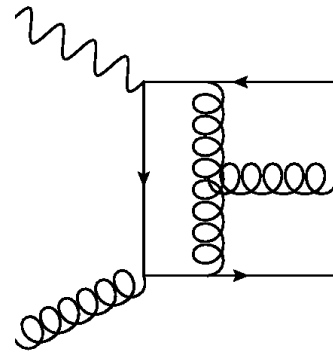
Eur.Phys.J.C75 (2015) 2

DIS jet production in NNLO

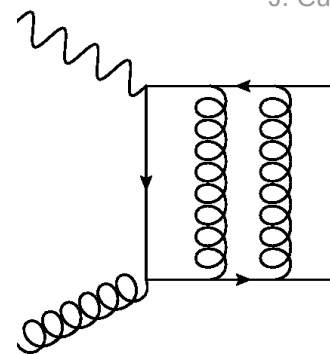
J. Currie, et al. [RPL 117 (2016) 042001]
 J. Currie, et al. [JHEP 1707 (2017) 018]



Double-real



Real-virtual



Double-virtual

$$d\sigma_{NNLO}^{RR,S} \approx \underbrace{X(\{p_X\})}_{\text{antenna}} \underbrace{d\Phi_3(\{p_X\})}_{\text{Antenna PS}} \times \underbrace{|\mathcal{M}(\{\tilde{p}_m\})|^2}_{\text{reduced ME}} \underbrace{d\Phi_m(\{\tilde{p}_m\})}_{\text{reduced PS}} \times \underbrace{\mathcal{J}(\{\tilde{p}_m\})}_{\text{jet function}}$$

A bit of history

- 1973 asymptotic freedom of QCD
 [PRL 30(1973) 1343 & 1346]
- 1993 NLO studies of DIS jet cross sections
 [Phys. Rev. D49 (1994) 3291]
- 2016 NNLO corrections for DIS jets
 [Phys. Rev. Lett. 117 (2016) 042001], [arXiv:1703.05977]

Antenna subtraction

- Cancellation of IR divergences with local subtraction terms
- Construction of (local) counter terms
- Move IR divergences across different phase space multiplicities

Scale dependence of NNLO cross sections

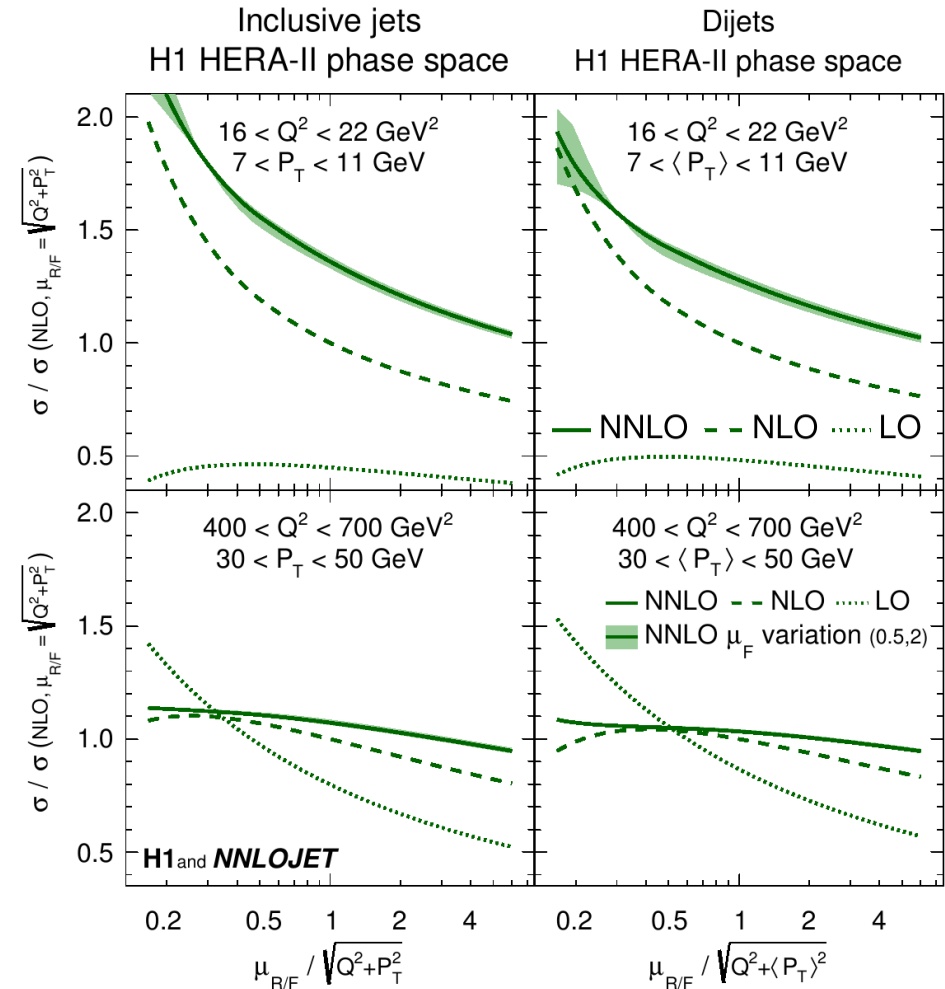
Simultaneous variation of μ_R and μ_F

At lower scales

- Significant NNLO k-factors
- NNLO with reduced scale dependence
- Inclusive jets with higher scale dependence than dijets

At higher scales

- NNLO with reduced scale dependence
- μ_F dependence very small



α_s -fit methodology

α_s determined in χ^2 -minimisation

- $\alpha_s(m_Z)$ is a free parameter to NNLO theory prediction σ_i

$$\chi^2 = \sum_{i,j} \log \frac{S_i}{\sigma_i} (V_{\text{exp}} + V_{\text{had}} + V_{\text{PDF}})^{-1}_{ij} \log \frac{S_j}{\sigma_j}$$

S_i	H1 jet data
σ_i	NNLO theory
V	covariance matrices

- NNLO theory is sensitive to $\alpha_s(m_Z)$

$$\sigma_i = \sum_{n=1}^{\infty} \sum_{k=g,q,\bar{q}} \int dx f_k(x, \mu_F) \hat{\sigma}_{i,k}^{(n)}(x, \mu_R, \mu_F) \cdot C_{\text{had}}$$

Hard ME's

$$\hat{\sigma}_{i,k}^{(n)} = \alpha_s^n(\mu_R) \tilde{\sigma}_{i,k}^{(n)}(x, \mu_R, \mu_F)$$

- α_s dependence of PDF is accounted for by using $\mu_{F,0}=20\text{GeV}$ and applying DGLAP

PDFs $\frac{\partial f}{\partial \alpha_s} = \frac{\mathcal{P} \otimes f}{\beta}$

Perform fits to

- All inclusive jet data sets (137 data points)
- All dijet data sets (103 data points)
- All H1 jet data taken together (denoted as 'H1 jets')
(exclude HERA-I dijet data as correlations to inclusive jets are not known)

Strong coupling in NNLO from jets

α_s from individual data sets

- High experimental precision
- Scale uncertainty is largest (theory) error
- All fits with good χ^2
-> consistency of data

Main result

- Inclusive jets & dijets
 $\mu > 28 \text{ GeV}$, 91 data points

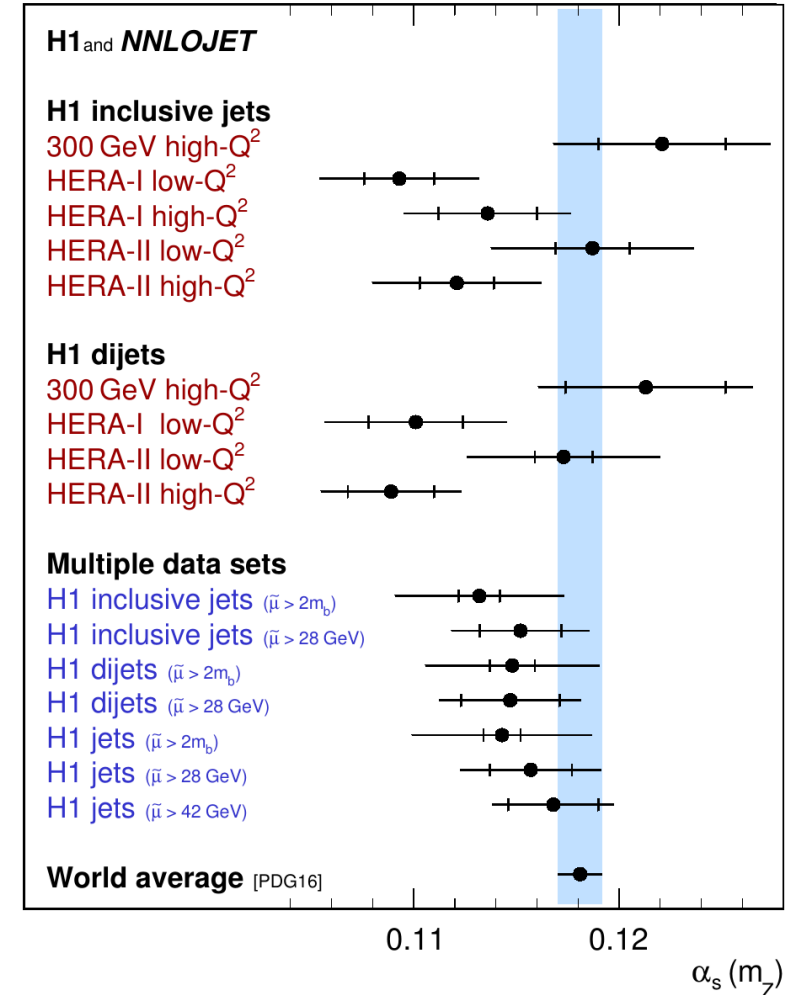
$$\alpha_s(m_Z) = 0.1157 (20)_{\text{exp}} (6)_{\text{had}} (3)_{\text{PDF}} (2)_{\text{PDF}\alpha_s} (3)_{\text{PDFset}} (27)_{\text{scale}}$$

- Moderate exp. precision (due to $\mu > 28 \text{ GeV}$)
- Scale uncertainty dominates
- PDF uncertainties negligible

Smallest exp. uncertainty

- Fit to all data: $\Delta\alpha_s = (9)_{\text{exp}}$

α_s results from H1 jet data in NNLO



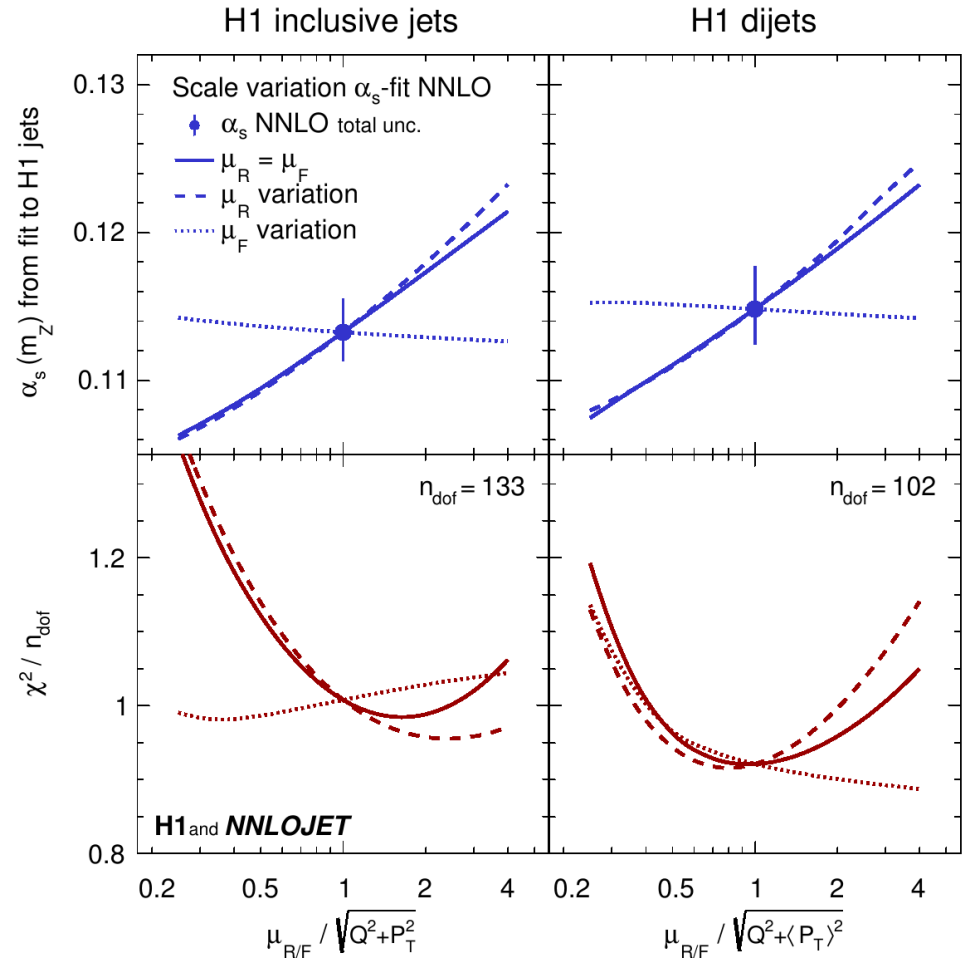
Scale dependence of α_s fit

α_s results as a function of scale factors

- Smooth results for studied scale variations
- μ_R variation with more impact than μ_F

χ^2 values

- somewhat a 'technical parameter'
-> not intended to be a parabolas
- χ^2 values increase for large scale factors
-> large scale factors disvafored



Scale choice for α_s fit

Study scales calculated from Q^2 and p_T

' p_T ' refers to: p_{T}^{jet} or $\langle p_T \rangle$

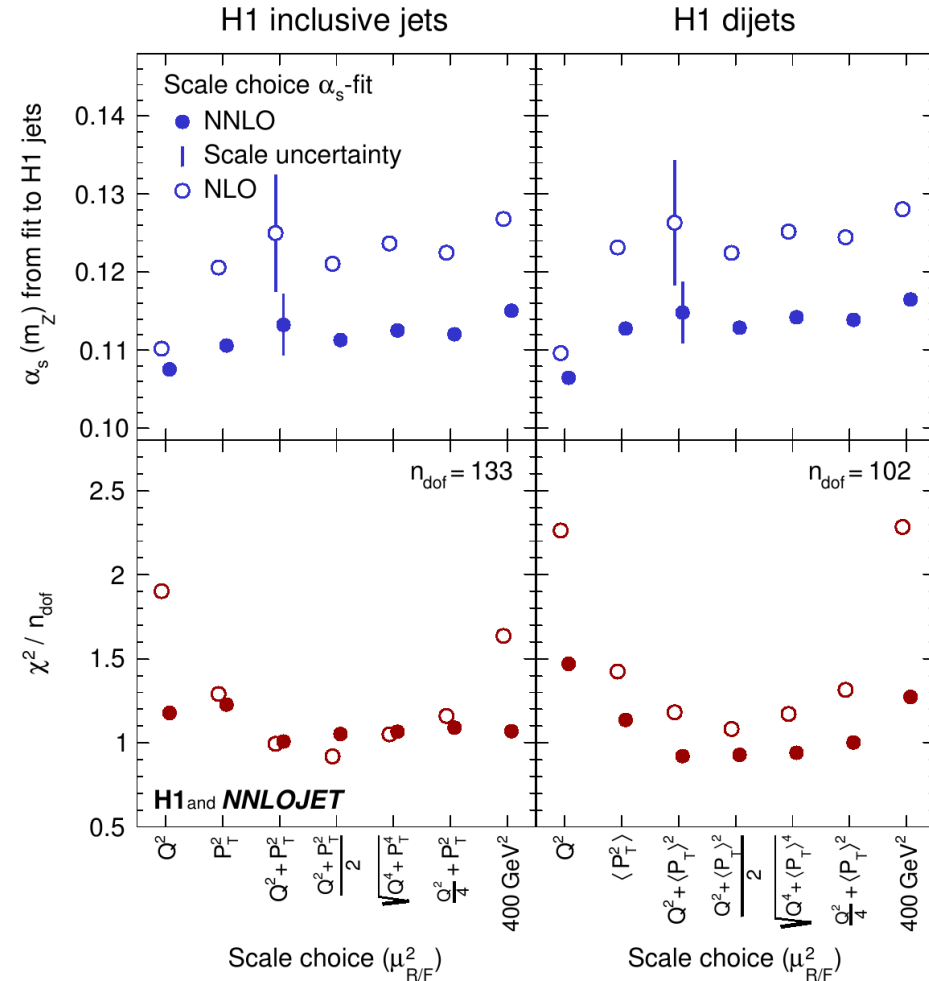
α_s results and χ^2 values

- Spread of results covered by scale uncertainty
- χ^2 values are similar for different choices
-> NNLO with small 'scale dependence'

NLO matrix elements

- Large scale uncertainty
- Relevant dependence of result on scale choice
- Mainly larger χ^2 values than NNLO
- Larger fluctuation of χ^2 values than NNLO

NNLO with reduced scale dependence



Dependence on the PDF

PDF is an external input to NNLO calculation

PDF fitting groups differ

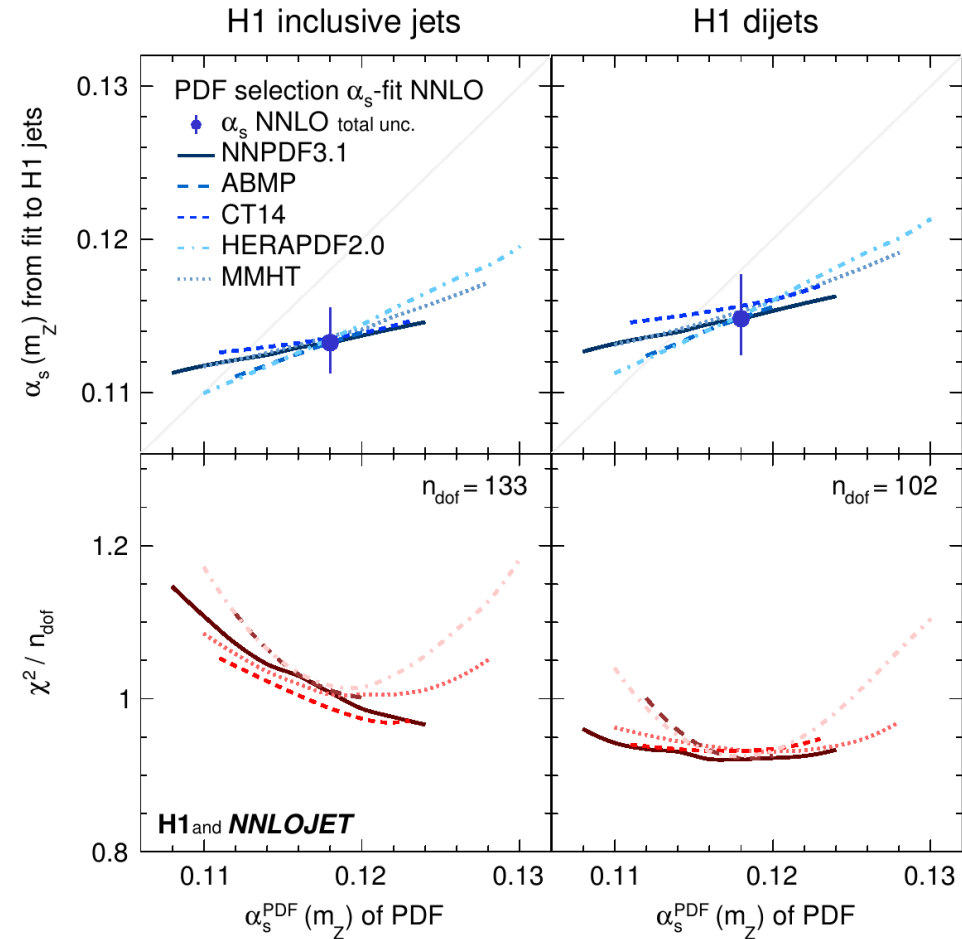
- choice of input data sets, PDF parameterisations, model parameters, fit methodology, etc...
- Though: different PDFs appear to be quite consistent

Choice of α_s for PDF determination

- $\alpha_s^{\text{PDF}}(m_Z)$ important input parameter to PDF fit
- Small correlation with fitted results

Our (main) α_s result

- almost independent on PDF assumptions



Comparison of NNLO predictions with data

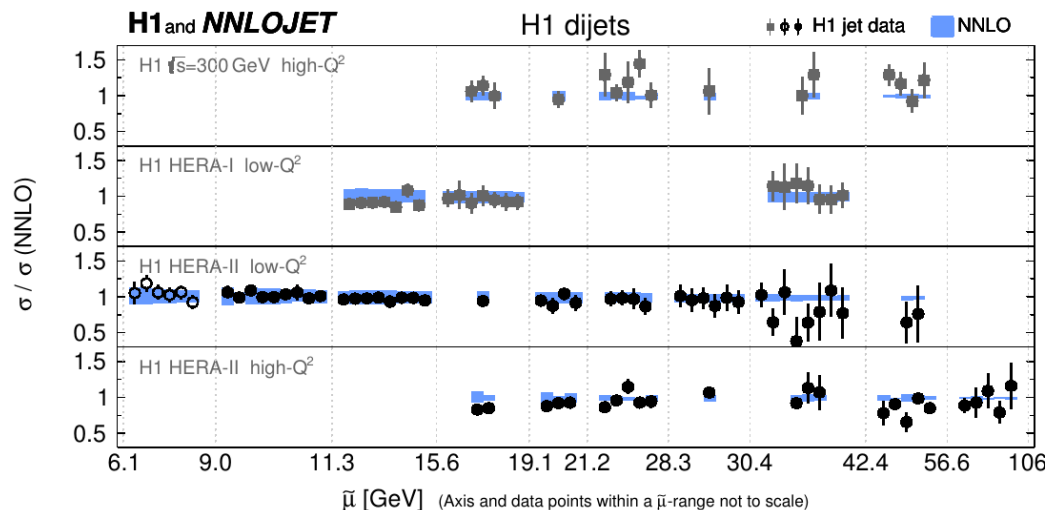
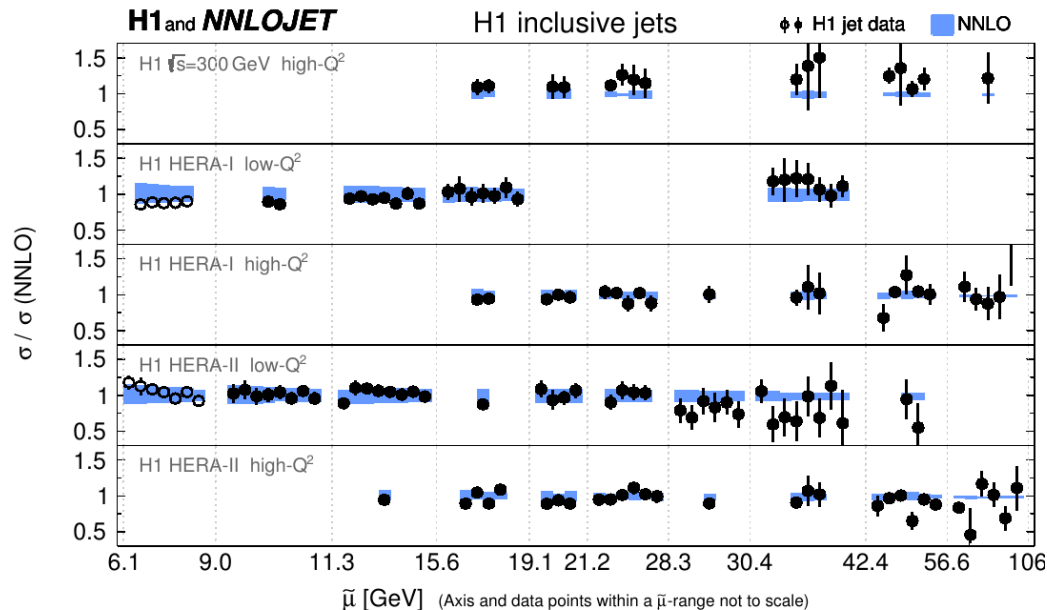
All H1 jet cross section data compared to NNLO predictions

- Inclusive jets
- Dijets

Overall good agreement

- NNLO describes all data very well
- Also justified of course by good χ^2 values of the fits

Great success of pQCD



Tests of running of strong coupling

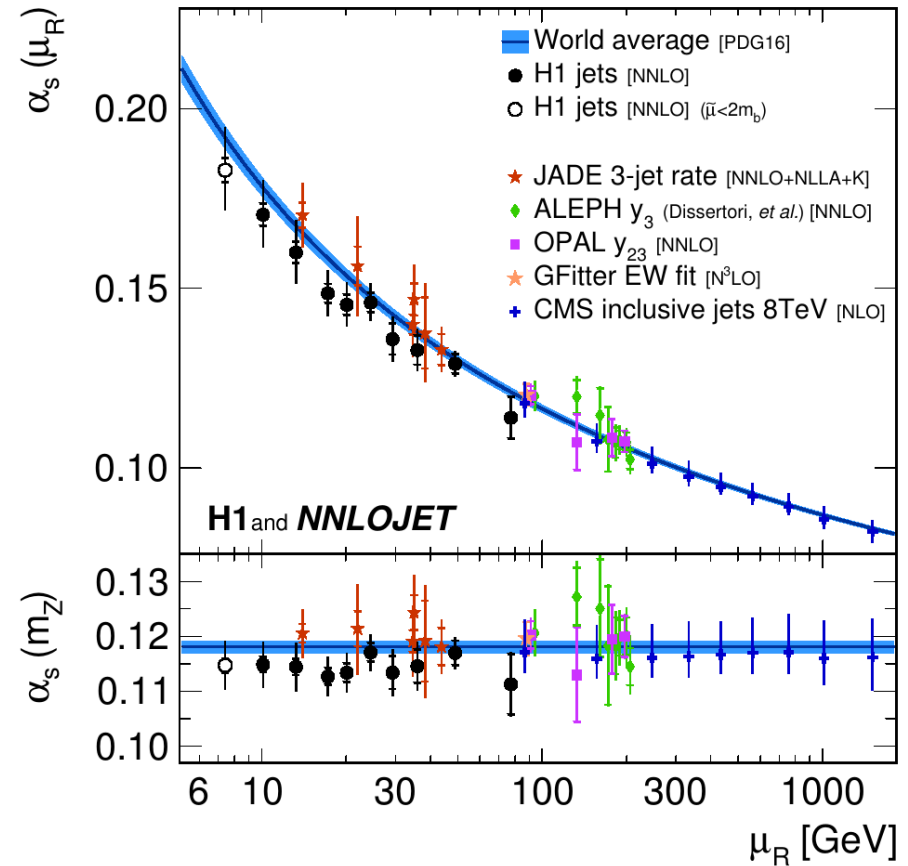
Test running of strong coupling

- Perform fits to groups of data points at similar scale
- Assumes running to be valid within the limited range covered by interval
- All fits have good χ^2

Results

- Consistency with expectation at all scales
- Scale uncertainty dominates at lower μ
- Consistency of inclusive jets and dijets (backup)

Most precise test in range $7 < \mu < 90$ GeV



Alternative α_s fitting approach

'PDF+ α_s -fit'
H1PDF2017

Alternative α_s fitting approach: 'PDF+ α_s -fit'

Simultaneous fit PDFs and α_s

- PDFs are predominantly determined from H1 inclusive DIS data

Perform H1 alone PDF fit: **H1PDF2017**

- Use (all) H1 inclusive DIS data
 - Use (all) H1 normalised jet cross section data
- > 1529 data points

Normalised jet cross sections

- Jet cross sections normalised to inclusive DIS
- Correlations of jets and inclusive DIS cancel

PDFs are parameterised as

$$xf(x)|_{\mu_0} = f_A x^{f_B} (1-x)^{f_C} (1 + f_D x + f_E x^2)$$

Cross section: $\sim \text{PDF} \otimes \sigma$

$$\sigma_i = \sum_{k=g,q,\bar{q}} \int dx f_k(x, \mu_F) \hat{\sigma}_{i,k}(x, \mu_R, \mu_F) \cdot C_{\text{had},i}$$

Normalised jets

Data set [ref.]	Q^2 domain	Inclusive jets	Dijets	Normalised inclusive jets	Normalised dijets	Stat. corr. between samples
300 GeV [17]	high- Q^2	✓	✓	-	-	-
HERA-I [23]	low- Q^2	✓	✓	-	-	-
HERA-I [21]	high- Q^2	✓	-	✓	-	-
HERA-II [15]	low- Q^2	✓	✓	✓	✓	✓
HERA-II [15, 24]	high- Q^2	✓	✓	✓	✓	✓

Inclusive NC & CC DIS

Data set [ref.]	Lepton type	\sqrt{s} [GeV]	Q^2 range [GeV ²]	NC cross sections	CC cross sections	Lepton beam polarisation
Combined low- Q^2 [64]	e^+	301,319	(0.5) 12 - 150	✓	-	-
Combined low- E_p [64]	e^+	225,252	(1.5) 12 - 90	✓	-	-
94 - 97 [61]	e^+	301	150 - 30 000	✓	✓	-
98 - 99 [62, 63]	e^-	319	150 - 30 000	✓	✓	-
99 - 00 [63]	e^+	319	150 - 30 000	✓	✓	-
HERA-II [65]	e^+	319	120 - 30 000	✓	✓	✓
HERA-II [65]	e^-	319	120 - 50 000	✓	✓	✓

PDF+ α_s -fit – H1PDF2017 [NNLO]

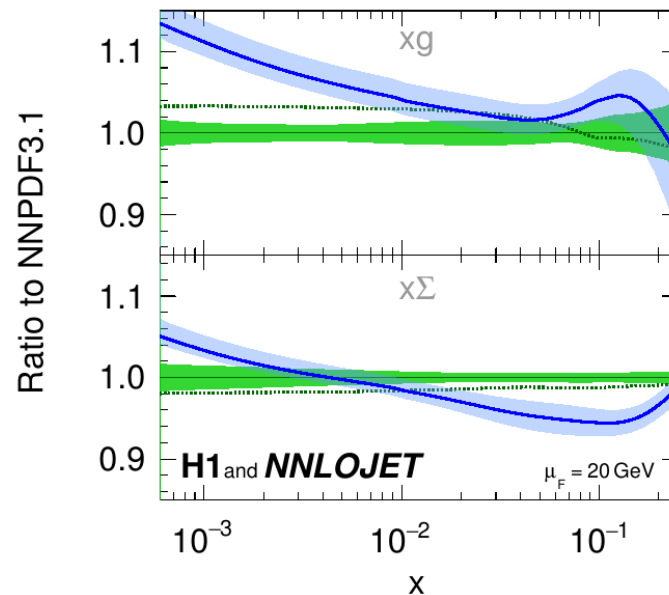
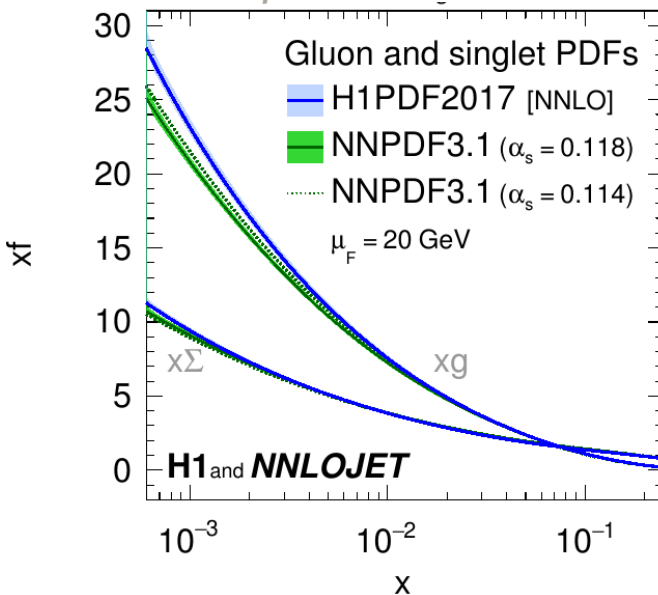
Result for PDFs

- Set of PDFs determined with high precision
- Despite α_s is a free parameter to the fit: precision is competitive with global PDF fitters
- Gluon at lower x -values tends to be higher
-> nowadays: also favored by small- x resummed PDFs

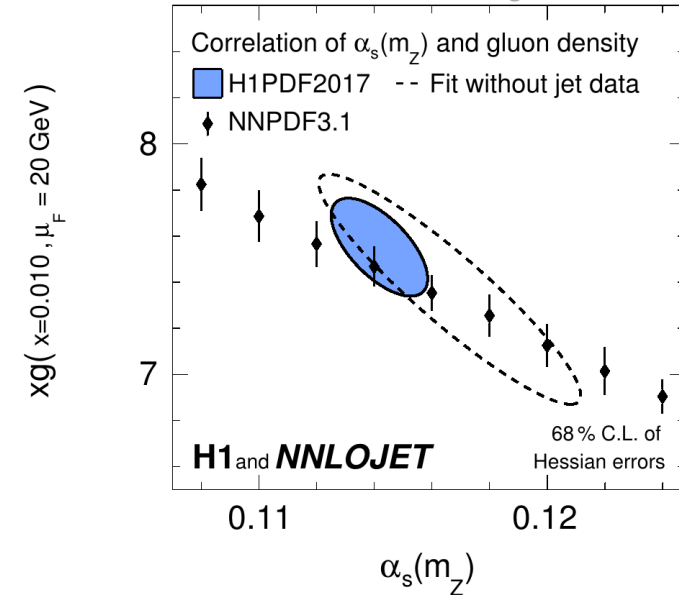
PDF+ α_s -fit

- Using H1 jet data allows a precise determination of the gluon PDF and α_s
- $\chi^2/\text{ndf} \sim 1.01$

Comparison of H1PDF2017 and NNPDF3.1



Correlation of α_s and g



Results

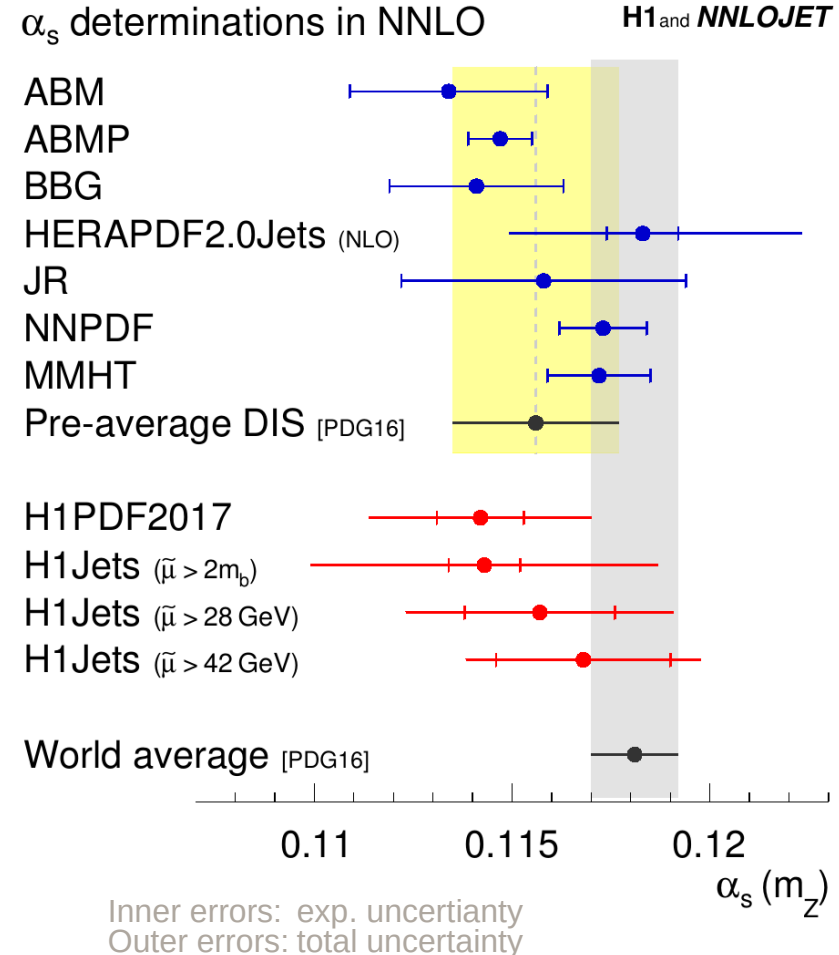
α_s determined in PDF+ α_s -fit

$$\alpha_s(m_Z) = 0.1142 (11)_{\text{exp,had,PDF}} (2)_{\text{mod}} (2)_{\text{par}} (26)_{\text{scale}}$$

- High experimental precision
- Moderate theory uncertainty from NNLO

Comparison

- Higher precision than most of other (comparable) determinations
 - > PDF groups commonly determine exp. uncertainties (only)
 - > We further estimate scale uncertainties
- All H1 results consistent
- Results competitive with world average
- All results from DIS data tend to be lower than world average value



Summary

All H1 jet data confronted with NNLO predictions

- NNLO provides improved description w.r.t. NLO
- Quantitative comparison of all data
- NNLO predictions studied in great detail

NNLO used for determination of $\alpha_s(m_Z)$

- α_s -fit $\alpha_s(m_Z) = 0.1157 (20)_{\text{exp}} (6)_{\text{had}} (3)_{\text{PDF}} (2)_{\text{PDF}\alpha_s} (3)_{\text{PDFset}} (27)_{\text{scale}}$
- α_s +PDF-fit $\alpha_s(m_Z) = 0.1142 (11)_{\text{exp,had,PDF}} (2)_{\text{mod}} (2)_{\text{par}} (26)_{\text{scale}}$
- High experimental and theoretical precision

NNLO predictions for jets are used for PDF fits for the first time

- Successful determination of gluon-density and $\alpha_s(m_Z)$ simultaneously
- Competitive precision of PDFs and $\alpha_s(m_Z)$
- H1PDF2017 available at LHAPDF

Fruitful collaboration of theoreticians and experimentalists (H1 & NNLOJET)

Study of total uncertainty

Scale uncertainties at various scales μ

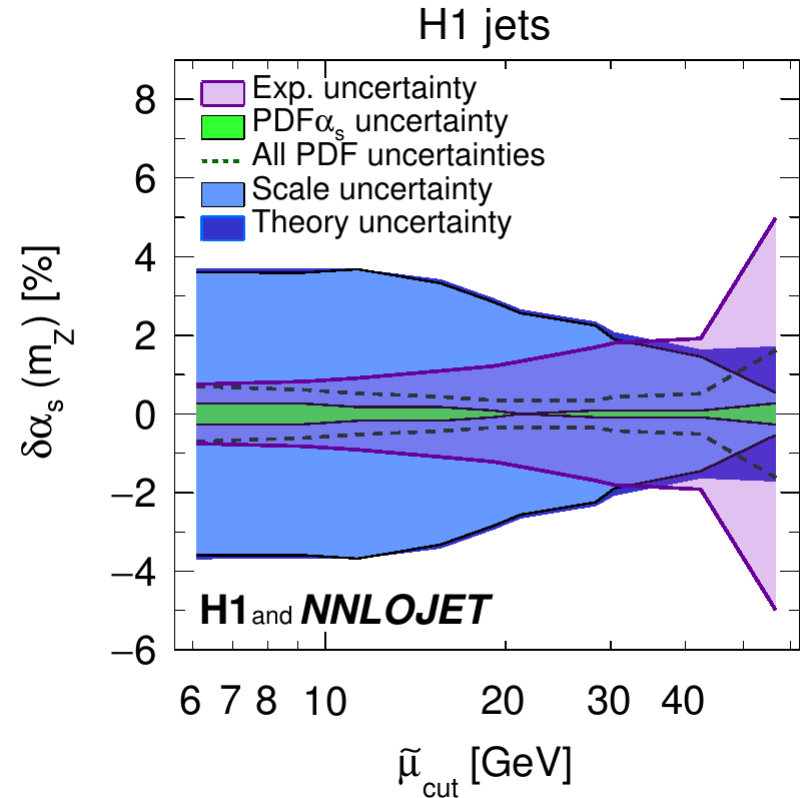
- At low- μ : large scale uncertainties...
- ... but also high sensitivity to $\alpha_s(m_Z)$

Fits imposing a cut on scale μ

- Repeat α_s fits:
successively cut away data below μ_{cut}

Results

- Scale uncertainty decreases with μ_{cut}
- Exp. uncertainty increases with μ_{cut}



Cut on μ can balance between exp. and theoretical uncertainties at constant total precision

$\alpha_s(m_Z)$ dependence of cross sections

Jet cross sections directly sensitive to α_s

$$\sigma_i = \sum_{n=1}^{\infty} \sum_{k=g,q,\bar{q}} \int dx f_k(x, \mu_F) \hat{\sigma}_{i,k}^{(n)}(x, \mu_R, \mu_F) \cdot C_{\text{had}}$$

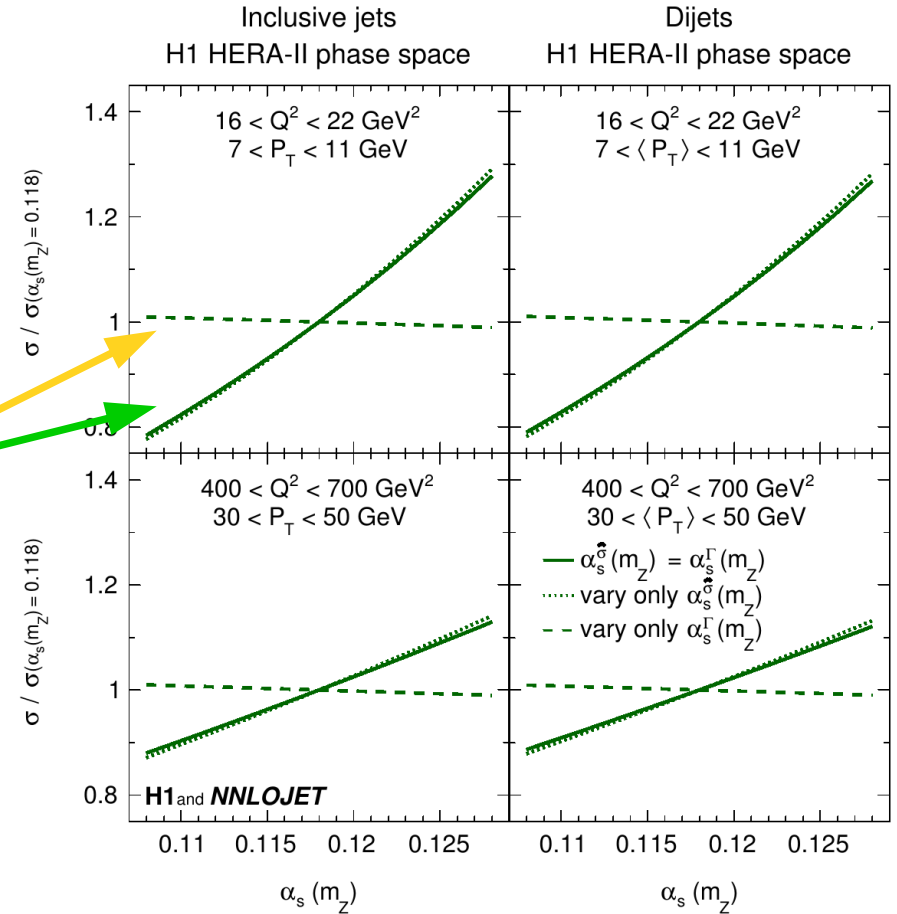
Two α_s -dependencies

PDFs $\frac{\partial f}{\partial \alpha_s} = \frac{\mathcal{P} \otimes f}{\beta}$

Hard ME's

$$\hat{\sigma}_{i,k}^{(n)} = \alpha_s^n(\mu_R) \tilde{\sigma}_{i,k}^{(n)}(x, \mu_R, \mu_F)$$

- *PDF's with almost negligible sensitivity*
- *PDF's with almost negligible sensitivity*



α_s dependencies separately fitted

Fits to

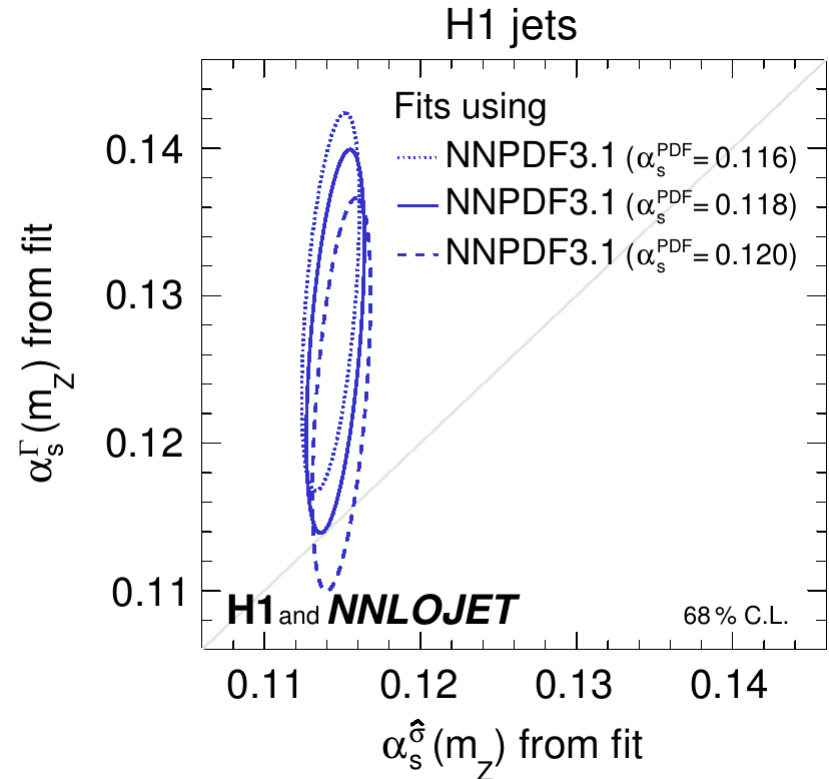
- Inclusive jet and dijet data fitted together
- Fits performed for different PDFs

Fits with two free α_s parameters

$$\sigma_i = f(\alpha_s^f(m_Z)) \otimes \hat{\sigma}_k(\alpha_s^{\hat{\sigma}}(m_Z)) \cdot c_{\text{had}}$$

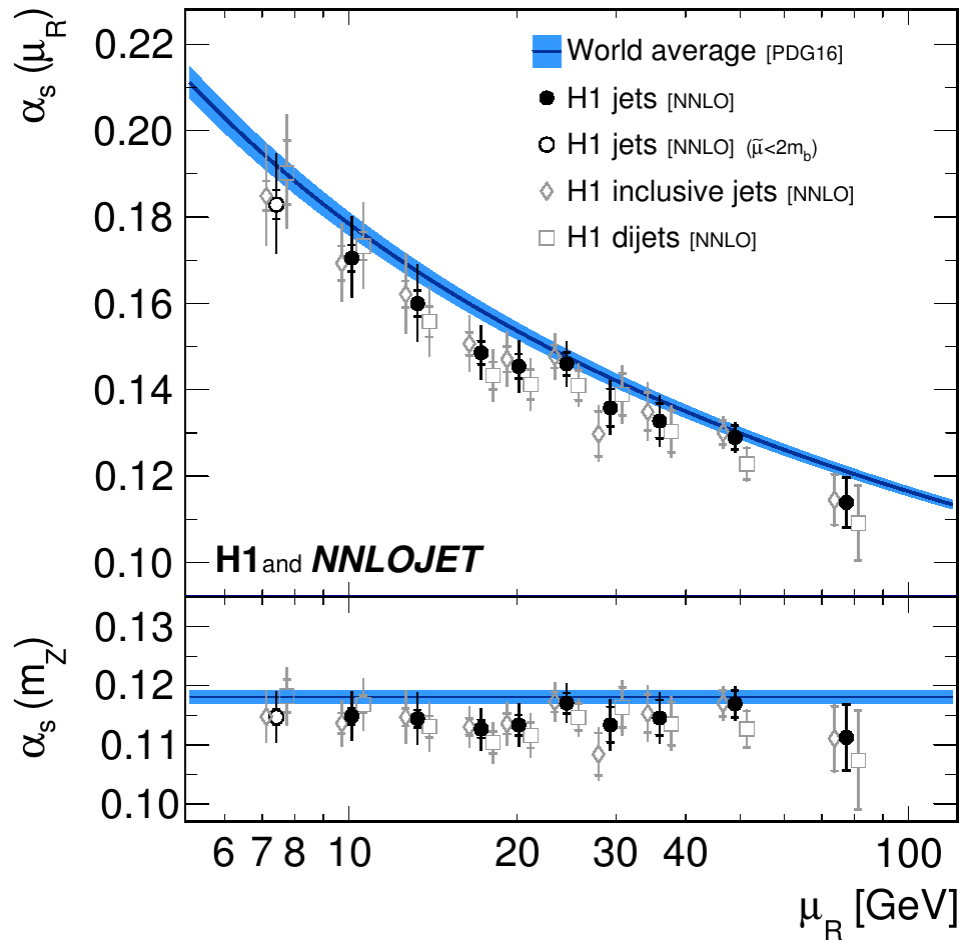
Results

- Most sensitivity arises from **matrix elements**
- Best-fit α_s -values in **PDF's** and **ME's** are consistent
- Anti-correlation between $\alpha_s^{\text{PDF}}(m_Z)$ and $\alpha_s^{\Gamma}(m_Z)$



$\alpha_s(m_Z)$ values from H1 jet cross sections

Data	$\tilde{\mu}_{\text{cut}}$	$\alpha_s(m_Z)$ with uncertainties	th	tot	χ^2/n_{dof}
Inclusive jets					
300 GeV high- Q^2	$2m_b$	0.1221 (31) _{exp} (22) _{had} (5) _{PDF} (3) _{PDFα_s} (4) _{PDFset} (36) _{scale}	(43) _{th}	(53) _{tot}	6.5/15
HERA-I low- Q^2	$2m_b$	0.1093 (17) _{exp} (8) _{had} (5) _{PDF} (5) _{PDFα_s} (7) _{PDFset} (33) _{scale}	(35) _{th}	(39) _{tot}	17.5/22
HERA-I high- Q^2	$2m_b$	0.1136 (24) _{exp} (9) _{had} (6) _{PDF} (4) _{PDFα_s} (4) _{PDFset} (31) _{scale}	(33) _{th}	(41) _{tot}	14.7/23
HERA-II low- Q^2	$2m_b$	0.1187 (18) _{exp} (8) _{had} (4) _{PDF} (4) _{PDFα_s} (3) _{PDFset} (45) _{scale}	(46) _{th}	(50) _{tot}	29.6/40
HERA-II high- Q^2	$2m_b$	0.1121 (18) _{exp} (9) _{had} (5) _{PDF} (4) _{PDFα_s} (2) _{PDFset} (35) _{scale}	(37) _{th}	(41) _{tot}	42.5/29
Dijets					
300 GeV high- Q^2	$2m_b$	0.1213 (39) _{exp} (17) _{had} (5) _{PDF} (2) _{PDFα_s} (3) _{PDFset} (31) _{scale}	(35) _{th}	(52) _{tot}	13.6/15
HERA-I low- Q^2	$2m_b$	0.1101 (23) _{exp} (8) _{had} (5) _{PDF} (4) _{PDFα_s} (5) _{PDFset} (36) _{scale}	(38) _{th}	(45) _{tot}	10.4/20
HERA-II low- Q^2	$2m_b$	0.1173 (14) _{exp} (9) _{had} (5) _{PDF} (5) _{PDFα_s} (3) _{PDFset} (44) _{scale}	(45) _{th}	(47) _{tot}	17.4/41
HERA-II high- Q^2	$2m_b$	0.1089 (21) _{exp} (7) _{had} (5) _{PDF} (3) _{PDFα_s} (3) _{PDFset} (25) _{scale}	(27) _{th}	(34) _{tot}	28.0/23
H1 inclusive jets	$2m_b$	0.1132 (10) _{exp} (5) _{had} (4) _{PDF} (4) _{PDFα_s} (2) _{PDFset} (40) _{scale}	(40) _{th}	(42) _{tot}	134.0/133
H1 inclusive jets	28 GeV	0.1152 (20) _{exp} (6) _{had} (2) _{PDF} (2) _{PDFα_s} (3) _{PDFset} (26) _{scale}	(27) _{th}	(33) _{tot}	44.1/60
H1 dijets	$2m_b$	0.1148 (11) _{exp} (6) _{had} (5) _{PDF} (4) _{PDFα_s} (4) _{PDFset} (40) _{scale}	(41) _{th}	(42) _{tot}	93.9/102
H1 dijets	28 GeV	0.1147 (24) _{exp} (5) _{had} (3) _{PDF} (2) _{PDFα_s} (3) _{PDFset} (24) _{scale}	(25) _{th}	(35) _{tot}	30.8/43
H1 jets	$2m_b$	0.1143 (9) _{exp} (6) _{had} (5) _{PDF} (5) _{PDFα_s} (4) _{PDFset} (42) _{scale}	(43) _{th}	(44) _{tot}	195.0/199
H1 jets	28 GeV	0.1157 (20) _{exp} (6) _{had} (3) _{PDF} (2) _{PDFα_s} (3) _{PDFset} (27) _{scale}	(28) _{th}	(34) _{tot}	63.2/90
H1 jets	42 GeV	0.1168 (22) _{exp} (7) _{had} (2) _{PDF} (2) _{PDFα_s} (5) _{PDFset} (17) _{scale}	(20) _{th}	(30) _{tot}	37.6/40
H1PDF2017 [NNLO]	$2m_b$	0.1142 (11) _{exp,NP,PDF} (2) _{mod} (2) _{par} (26) _{scale}		(28) _{tot}	1539.7/1516



Data set [ref.]	\sqrt{s} [GeV]	\mathcal{L} [pb ⁻¹]	DIS kinematic range	Inclusive jets	Dijets $n_{\text{jets}} \geq 2$
300 GeV [17]	300	33	$150 < Q^2 < 5000 \text{ GeV}^2$ $0.2 < y < 0.6$	$7 < P_{\text{T}}^{\text{jet}} < 50 \text{ GeV}$	$P_{\text{T}}^{\text{jet}} > 7 \text{ GeV}$ $8.5 < \langle P_{\text{T}} \rangle < 35 \text{ GeV}$
HERA-I [23]	319	43.5	$5 < Q^2 < 100 \text{ GeV}^2$ $0.2 < y < 0.7$	$5 < P_{\text{T}}^{\text{jet}} < 80 \text{ GeV}$	$5 < P_{\text{T}}^{\text{jet}} < 50 \text{ GeV}$ $5 < \langle P_{\text{T}} \rangle < 80 \text{ GeV}$ $m_{12} > 18 \text{ GeV}$ $(\langle P_{\text{T}} \rangle > 7 \text{ GeV})^*$
HERA-I [21]	319	65.4	$150 < Q^2 < 15000 \text{ GeV}^2$ $0.2 < y < 0.7$	$5 < P_{\text{T}}^{\text{jet}} < 50 \text{ GeV}$	–
HERA-II [15]	319	290	$5.5 < Q^2 < 80 \text{ GeV}^2$ $0.2 < y < 0.6$	$4.5 < P_{\text{T}}^{\text{jet}} < 50 \text{ GeV}$	$P_{\text{T}}^{\text{jet}} > 4 \text{ GeV}$ $5 < \langle P_{\text{T}} \rangle < 50 \text{ GeV}$
HERA-II [15, 24]	319	351	$150 < Q^2 < 15000 \text{ GeV}^2$ $0.2 < y < 0.7$	$5 < P_{\text{T}}^{\text{jet}} < 50 \text{ GeV}$	$5 < P_{\text{T}}^{\text{jet}} < 50 \text{ GeV}$ $7 < \langle P_{\text{T}} \rangle < 50 \text{ GeV}$ $m_{12} > 16 \text{ GeV}$

Inclusive jet cross sections

Inclusive jet cross sections

- low Q^2 : $4.5 < P_T < 50$ GeV
- high Q^2 : $5 < P_T < 50$ GeV

Predictions

- NLO, aNNLO & NNLO

NLO

- Data well described within uncertainties

aNNLO

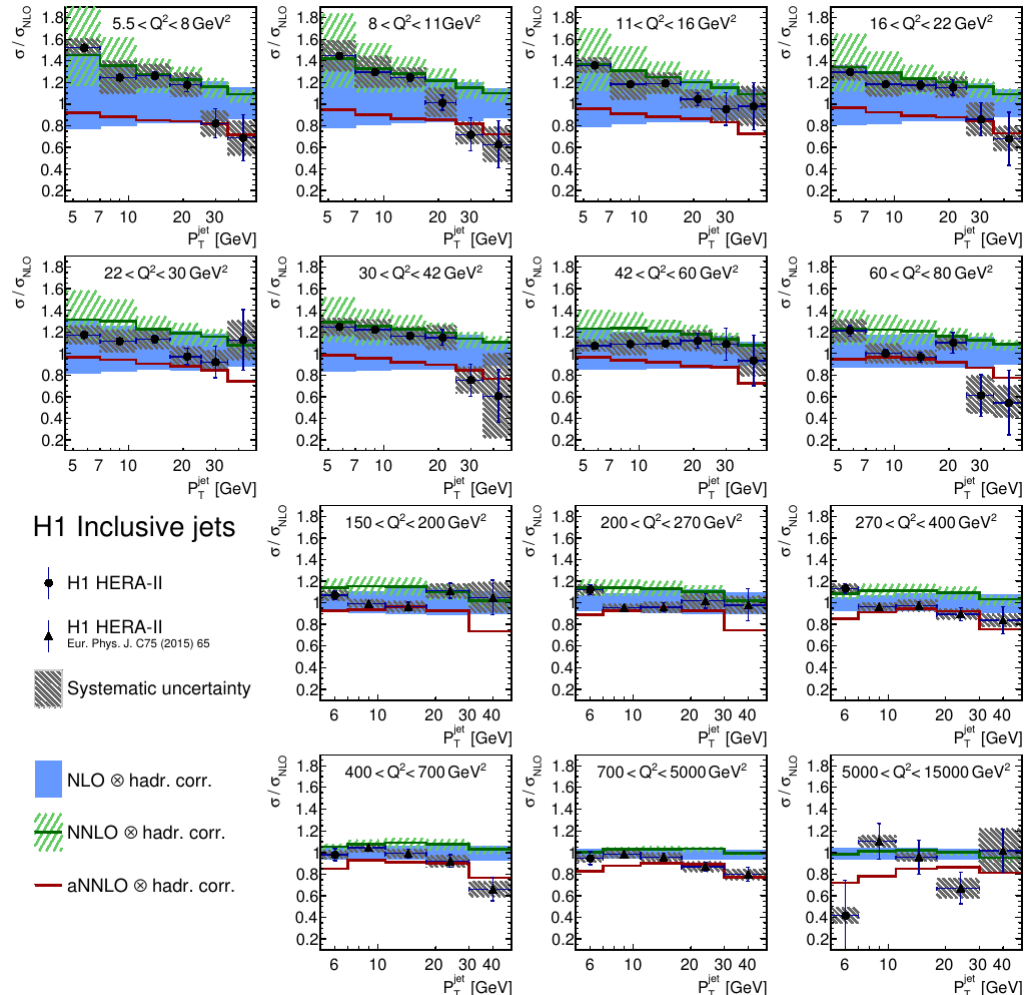
- Somewhat improved shape description

NNLO

- Improved shape and normalisation
- Reduced scale uncertainties for larger values of μ_r

Also measured

- Normalised inclusive jet cross sections



Ratio of dijet cross sections to NLO

Scale uncertainty

- So-called '7-point scale variation': Vary μ_r and μ_f independently by factors of 2 and 0.5, but exclude variations in 'opposite' directions

Ratio to NLO prediction

- NLO give reasonable descriptions within large scale uncertainties
- aNNLO improves shape
 - aNNLO expected to improve description at high $\langle p_T \rangle$
- NNLO improves shape dependence
 - NNLO predictions have smaller scale uncertainties than NLO at high- $\langle p_T \rangle$

